Auditory and Vestibular Research

Hyperspectral Imaging Tympanoscope: System Development and preliminary Study for Assessment of Its Potential as a Diagnostic Tool

Tayebe Taghizade[1], Saeid Farahani[1*], Ali kouhi[2 3] , Ali Balooch[4], Alireza Akbarzade-baghban[5] , Mohammad Esmaili[6]

[1] Department of Audiology, Faculty of Rehabilitation, Tehran University of Medical Sciences, Tehran, Iran
[2] Department of Otolaryngology Head and Neck Surgery, Amir A'lam Hospital, Tehran University of Medical Sciences, Tehran, Iran
[3] Otorhinolaryngology Research Center, Tehran University of Medical Sciences, Tehran, Iran
[4] Noorimentajhiz Company, Science and Technology Park, Kashan, Iran
[5] Proteomics Research Center, Department of Biostatistics, School of Allied Medical Sciences, Shahid Beheshti University of Medical Sciences, Tehran, Iran
[6] Municipality Organization, Qom, Iran

[*]Correspondence: Saeid Farahani , S_farahani@tums.ac.ir

Orcid ID:
Tayebe Taghizade: 0009-0003-2720-5022
Saeid Farahani: https://orcid.org/0000-0003-2541-283X
Ali kouhi: 0000-0002-4154-8908
Ali Balooch: 0009-0000-5239-7175
Alireza Akbarzade-baghban: 0000-0002-0961-1874
Mohammad Esmaili: 0009-0006-3419-1492

Highlights:
The hyperspectral tympanoscope is a nowel diagnostic imaging method for detecting MEE.
The hyperspectral tympanoscope is a cost-effective tool for diagnosing MEE.
NIR imaging could quantitatively distinguish between the presence or absence of fluid.

Abstract:
Background and Aim: Accurate diagnosis of middle ear effusion (MEE) remains one of the most challenging tasks in the medical field due to the lack of reliable diagnostic tools available to physicians and audiologists. This study aimed to design and develop a hyperspectral imaging tympanoscope for diagnosing MEE as the first phase, focusing on system design and preliminary evaluation in a small sample.
Methods: The tympanoscope system was constructed using an ear endoscope, lens, camera, and near-infrared wavelength, and its performance was evaluated with a middle ear-mimicking phantom. Additionally, a preliminary study was conducted on middle ear images from ten children—five healthy and five diagnosed with MEE.
Results: Results from the phantom experiments demonstrated that the Weber contrast difference between phantoms with and without fluid in visible otoscopy and hyperspectral tympanoscopy was 0.16 and 0.49, respectively. As a result, in hyperspectral tympanoscopy, the contrast difference between fluid presence and absence was nearly tripled. Furthermore, in the preliminary human study, significant difference was found in Weber contrast between healthy children and those with MEE ($p<0.001$), confirming higher contrast in the MEE group.
Conclusion: The hyperspectral imaging tympanoscope could quantitatively distinguish between the presence or absence of fluid in the middle ear and the developed system has potential as a diagnostic and monitoring tool for middle ear effusion.
Keywords: hyperspectral, tympanoscope, middle ear effusion, middle ear-mimicking phantom.

Introduction

Middle ear effusion (MEE) characterized by fluid accumulation in the middle ear cavity, often results from tympanic membrane infection [1-3]. It is the second most common disease diagnosed in children after acute upper respiratory tract infections with at least 80% experiencing one or more episodes by age three [4,5]. Diagnose primarily relies on otoscopy or endoscopy using a white light source to assess tympanic membrane (TM) color changes and mobility [6,7]. However, precisely diagnosis is challenging due to their overlapping symptoms, like inflammation and temporary hearing loss leading to significant dependence on examiner expertise [8]. Diagnostic instruments include the otoscope, video otoscope, pneumatic otoscope, tympanometry, acoustic reflex measurement and broadband tympanometry [9].

It is important to note that conventional examinations are subjective, with interpretation varying widely among physicians [6]. Error rates for diagnosing middle ear diseases using digital imaging with a traditional otoscope were reported as 50% for pediatricians and 27% for otolaryngologists [7]. Another study estimated the accuracy of otitis media diagnosis by U.S. pediatricians at 51%, resulting in overdiagnosis (false positives) in 26% of cases [4,9,10]. Conversely, MEE is often underestimated (false negatives) due to its asymptomatic nature and the limitations of conventional otoscopy [10]. Consequently, there is a need for tools providing additional objective insights to improve diagnostic accuracy [7].

Most observations to date have concentrated on the visible wavelength range (400-700 nm), similar to conventional white light otoscopy [7]. This study's primary objective is to determine an appropriate near-infrared (NIR) wavelength capable of detecting tympanic membrane effusion with high sensitivity, offering a reliable diagnostic approach for MEE.

Hyperspectral imaging has demonstrated enhanced information for accurate disease detection compared to standard imaging (7,11-17). NIR wavelengths experience minimal attenuation at the TM, enabling greater light transmission and improved visualization of structures behind it. Kashani et al. developed a shortwave infrared (SWIR) otoscope for imaging middle ear structures and fluid within the SWIR region, predicting effusion presence with over 90% specificity and sensitivity [18]. It is worth mentioning that attenuation decreases considerably in the infrared (IR) and SWIR ranges, but imaging at these wavelengths requires specialized optics and photon detectors, substantially increasing device cost [8,9,]. Rajamanickam used a visual-NIR hyperspectral otoscope (600 nm to 1050 nm) for high-sensitivity fluid detection and precise diagnosis of middle ear infections, demonstrating peak contrast between ossicles and fluid at 1000 nm in a phantom model [9].

Therefore, we propose a hyperspectral imaging tympanoscope for visualizing middle ear structures and comparing healthy and infected states. This study aimed to develop and construct a portable hyperspectral imaging tympanoscope, providing physicians and audiologists with an objective, quantitative method to detect MEE presence, a condition currently diagnosed subjectively, focusing on system design and preliminary evaluation in a small sample.

Methods

Optical design

A hyperspectral imaging tympanoscope was developed using an ear endoscope. Endoscopes vary in tube length, diameter, and viewing angle (zero or 30 degrees). This study employed a 4 mm diameter, 10 cm length endoscope with a zero-degree angle for direct insertion into the ear canal. An integrated lens provides a clear display image with the power source located at the base. While white light is standard, this study used light-emitting diodes (LEDs) emitting specific wavelengths. A closed-circuit television (CCTV) lens (25 mm focal length) was positioned between the endoscope lens and the camera to project the eardrum image onto the camera detector. The camera, featuring a Sony IMX179 CCD sensor (resolution 3288x2512, 8-bit depth, frame rate up to 30 fps) captured the images. Figure 1A illustrates the schematic, while Figure 1B shows the final 3D-printed device. The body, designed in SolidWorks using 7000-series aluminum alloy, houses all components.

Based on a pilot study and previous data [7,9,18], wavelengths of 640 nm and 940 nm were initially selected for middle ear monitoring. The 940 nm wavelength was chosen because TM transparency increases at longer wavelengths compared to visible light, revealing details behind the TM more clearly [9,18]. Since silicon-based camera sensitivity extends to approximately 1000 nm, 940 nm was suitable. This wavelength can pass through the TM, reflects off structures behind it, and aids effusion detection. The 640 nm visible wavelength was used for comparison with NIR images in the phantom model.

Software

A LabVIEW code processed raw data from the tympanoscope and reconstructed images at the specified wavelength, saving them as JPEG files. Figure 2 shows the user interface, which allows gain and exposure time adjustment image saving in manual or timed modes. Using the digital tympanoscope, the TM position was visualized and adjusted before image capture. The software recorded and saved TM images on the monitor.

Preliminary study evaluation

The system's functionality was assessed by examining ten children (aged 3-12): five healthy controls and five diagnosed with unilateral MEE. This sample size is appropriate for a feasibility study, as similarly employed by Cavalcanti et al. [8] to assess early-stage device potential. MEE presence was verified through tympanometry and evaluation by two phisicians; any cerumen was removed. Procedures were explained to all participants, and informed consent was obtained. An expert audiologist fixed the child's head in a sitting position and captured NIR TM images using the hyperspectral tympanoscope. The endoscope was inserted until a clear closed TM image appeared on the monitor, standardizing the camera-to-TM distance across participants despite varying canal lengths.

Contrast, indicating pixel intensity variation across image regions is crucial for NIR imaging [9], which relies on differences between middle ear structures (e.g. ossicles, fluid). Weber contrast, defined as (I_max-I_min)/I_min (where I_max represents malleus intensity and I_min the background intensity) was measured at 940 nm for normal and infected ears [9]. To determine the Weber contrast, the intensity of the light reflected from the ossicle and air/effusion was recorded by creating a small box on different areas of the TM using image processing software as shown in Figure 3. The box determination was in accordance with the research conducted by Carr et al. [5]. Intensity normalization was used to maximize the intensity difference between different areas. For this purpose, the software set the pixel of the image with the highest and lowest intensity to 255 and 0, respectively, and in this way all pixels of the image were normalized based on intensity. Figure 3 depicts NIR images of the normal middle ear (Figure 3A) and the middle ear with effusion (Figure 3B). TM regions are marked: green (normal TM), red (TM with effusion), blue (malleus).

An independent samples t-test compared Weber contrast between groups. Data distribution normality was assessed using the Shapiro-Wilk test and variance equality was evaluated using Levene's test. All statistical analysis was performed in SPSS v.26.

Evaluation using a middle ear-mimicking phantom

A phantom replicating the ear canal, TM, malleus and middle ear cavity assessed the device's ability to detect and distinguish fluids behind a semitransparent membrane. The phantom was designed with SolidWorks software and manufactured using a 3D printer (Jahan 3D). It featured a 2 mL cubic cavity approximating human middle ear capacity. A latex medical glove rubber film (□0.18 mm thick), simulating TM properties [8]. Figure 4 details the phantom, including the model (Figure 4A) and the printed version utilized in this study (Figure 4B). The phantom is designed with two openings: a stretched latex sheet was secured to the front window and the manubrium was placed behind it. A cylinder (12 mm diameter, 25 mm length) coupled to this window simulated the ear canal. A second window facilitates the introduction of effusion-mimicking fluids into the middle ear model. Orange juice was selected for its optical similarity to MEE, as demonstrated in previous studies[5], although we acknowledge that it does not fully replicate the properties of real effusion. In addition, an empty phantom simulated a healthy middle ear. Images of empty and fluid-filled phantoms were captured at 640 nm and 940 nm for evaluation.

Results

Preliminary study results

The NIR imaging tympanoscope captured high resolution images of middle ear effusion at 940 nm. Comparing images from ten children (five healthy, mean age 6.2 years; five with MEE, mean age 6.4 years) revealed that the hyperspectral imaging tympanoscope visualized effusion typically undetectable due to limited visible light transmission through the TM.

Figure 5 displays Weber contrast values in normal and MEE cases. As reported by Schmilovitch et al., reflectance is lower from a TM affected by MEE, resulting in reduced intensities [19]. consequently, effusion

presence significantly increased the mean Weber contrast from 0.28(±0.02) to 0.56(±0.04). The Shapiro-wilk test confirmed normal data distribution in both groups ($p>0.05$). Levene's test showed no significant variance difference ($p>0.05$). The independent t-test (assuming equal variances) revealed a highly significant difference in Weber contrast between healthy children and those with MEE ($t(8)= 10.97$, $p<0.001$, CI-95=0.21,0.32), confirming higher contrast in the MEE group. Further, Cohen's effect size value ($d = 6.94$) suggested a huge practical significance. Although the effect size is very large, this is likely due to the small sample size and the selection of quite distinct samples in the two groups and intensity normalization; further validation in larger studies is needed.

Middle ear-mimicking phantom results

Imaging the 3D-printed phantom assessed fluid detection performance. Distinguishing empty and fluid-filled states under visible light was challenging, highlighting the difficulty of fluid detection with traditional otoscopy [9]. Therefore, NIR wavelengths were anticipated to provide superior optical contrast compared to visible imaging for detecting middle ear fluid.

The Weber contrast obtained from the phantom image with visible light when the phantom was empty and fluid-filled was 0.18 and 0.34, respectively. Also, The Weber contrast obtained from the phantom image with NIR light when the phantom was empty and fluid-filled was 0.16 and 0.65, respectively. As shown in Figure 6, the Weber contrast difference between phantoms with and without fluid in visible otoscopy and hyperspectral imaging tympanoscopy was 0.16 and 0.49, respectively. Thus, the contrast difference between fluid presence and absence was nearly tripled under NIR imaging. This enhanced contrast significantly aids physicians in detecting middle ear fluid.

Discussion

The hyperspectral imaging tympanoscope designed here offers a promising, cost-effective solution for detecting middle ear fluid. We demonstrated high sensitivity fluid detection in phantom models. While otoscopy remains the primary method for MEE observation, conventional visible light otoscopy has limited accuracy, with correct diagnosis rates of 46% for general practitioners, 51% for pediatricians, and 76% for otolaryngologists [5].

Previous research confirms reduced light attenuation at longer wavelengths [5]. Improved NIR transmission benefits otoscopy, as the light must penetrate the TM after reflecting off middle ear structures like the highly reflective ossicles and promontory before reaching the detector. Absorption or scattering by the TM reduces light reaching middle ear structures and further diminishes the reflected signal intensity returning to the detector, degrading contrast and resolution. The hyperspectral imaging approach depends on the contrast between different regions of the middle ear, such as the ossicles and fluid. For middle ear structures visible conventionally, the hyperspectral tympanoscope enhances their contrast [9].

The hyperspectral imaging tympanoscope exploits differential absorption between fluid-filled and empty middle ear regions. The significant NIR contrast generated assists clinicians in determining fluid presence. Overall, reflectance in fluid-filled areas is greater in the visible range and gradually decreases as the spectrum shifts toward the NIR region. NIR wavelengths exhibit minimal TM attenuation and greater transmission, improving visualization of structures behind the TM [8].

Kashani et al. constructed a SWIR otoscope to image the structures and fluid of the middle ear in 30 children undergoing tympanostomy tube surgery in the SWIR region. The results of their study showed that SWIR light creates better contrast between fluid-filled and air-filled spaces than visible light [18]. While attenuation decreases further in SWIR/IR regions, imaging requires costly specialized optics and photon detectors [9,18]. Therefore, this study utilized the NIR range to develop a cost-effective, highly sensitive hyperspectral imaging tympanoscope for MEE detection.

Our phantom results showed a greater contrast difference between fluid presence and absence under NIR imaging compared to visible otoscopy. Furthermore, the preliminary human study suggests hyperspectral tympanoscopy can detect MEE based on strong fluid absorption around 940 nm, yielding higher contrast in effusion images than in normal ears.

This report indicates the hyperspectral tympanoscope's potential as a nowel diagnostic imaging method for detecting MEE. Applying NIR light extends the usable spectrum to wavelengths where middle ear fluid contrast is significantly higher than in the visible range, enabling a more objective assessment of MEE presence. Objectifying this historically inconsistent diagnosis could minimize antibiotic overprescription and reduce

unnecessary tympanostomy tube surgeries, among the most commom pediatric procedures. However, the current findings are limited to system design and preliminary evaluation in a small sample; comprehensive clinical validation in larger populations will be reported in future phases. In future phases, the sensitivity, specificity, false positive and negative rates, predictive values, likelihood ratios, and kappa agreement coefficients will be evaluated. Additionally, artificial intelligence algorithms will be developed to enable automated detection of middle ear effusion.

Conclusion

This study designed a novel hyperspectral imaging tympanoscope and assessed its diagnostic potential for MEE using a phantom model and a preliminary human trial. Acquiring spectral images in the NIR range generated quantitative data to facilitate TM region differentiation. Phantom experiments confirmed the devices' ability to distinguish fluid-filled and empty middle ears. In the preliminary trial, images captured at 940 nm in ten children (five healthy and five with MEE) demonstrated the model's suitability for diagnosing middle ear diseases. However, confirming these findings requires a larger, detailed clinical study involving patients with conditions like acute otitis media and MEE, which remains future work. Additionally, this system could offer a cost-effective diagnostic solution for middle ear diseases in developing countries. As a future goal, integrating hyperspectral tympanoscopy with artificial intelligence algorithms could lead to automated diagnosis of MEE and could be used as a screening technique in settings where there are not enough specialists.

Ethical Considerations

Compliance with ethical guidelines

The experimental protocol was approved by the Ethical Committee of Tehran University of Medical Sciences with the document no. IR.TUMS.FNM.REC.1402.211.

Funding

This study was conducted under grant No.1403-2-103-72924 approved by Tehran Univesity of Medical Sciences.

Authors' contributions

TT: Conceptualization, design of the study, data collection, interpretation of the results, drafting the manuscript; SF: Conceptualization, interpretation of data and revision of the manuscript ; AK: Conceptualization and editing ; AB: Conceptualization, design and manufacture of the device ; AAB: Statistical analysis, ME: Conceptualization, design and manufacture of the device.

Conflict of interest

The authors declare that there is no conflict of interest regarding the publication of this paper.

Acknowledgments

We would like to thank the parents of the study community for their participation and the success of this project. We also thank the children who participated in the study.

References

1. Lieberthal AS, Carroll AE, Chonmaitree T, Ganiats TG, Hoberman A, Jackson MA, et al. The diagnosis and management of acute otitis media. Pediatrics. 2013;131(3):e964-99. [DOI:10.1542/peds.2012-3488]
2. Qureishi A, Lee Y, Belfield K, Birchall JP, Daniel M. Update on otitis media - prevention and treatment. Infect Drug Resist. 2014;7:15-24. [DOI:10.2147/IDR.S39637]
3. Sundvall PD, Papachristodoulou CE, Nordeman L. Diagnostic methods for acute otitis media in 1 to 12 year old children: a cross sectional study in primary health care. BMC Fam Pract. 2019;20(1):127. [DOI:10.1186/s12875-019-1018-4]
4. Abbott P, Rosenkranz S, Hu W, Gunasekera H, Reath J. The effect and acceptability of tympanometry and pneumatic otoscopy in general practitioner diagnosis and management of childhood ear disease. BMC Fam Pract. 2014;15:181. [DOI:10.1186/s12875-014-0181-x]
5. Carr JA, Valdez TA, Bruns OT, Bawendi MG. Using the shortwave infrared to image middle ear pathologies. Proc Natl Acad Sci U S A. 2016;113(36):9989-94. [DOI:10.1073/pnas.1610529113]
6. Valdez TA, Pandey R, Spegazzini N, Longo K, Roehm C, Dasari RR, Barman I. Multiwavelength fluorescence otoscope for video-rate chemical imaging of middle ear pathology. Anal Chem. 2014;86(20):10454-60. [DOI:10.1021/ac5030232]
7. Tran Van T, Lu Thi Thao M, Bui Mai Quynh L, Phan Ngoc Khuong C, Huynh Quang L. Application of Multispectral Imaging in the Human Tympanic Membrane. J Healthc Eng. 2020;2020:6219845. [DOI:10.1155/2020/6219845]

8. Cavalcanti TC, Kim S, Lee K, Lee SY, Park MK, Hwang JY. Smartphone-based spectral imaging otoscope: System development and preliminary study for evaluation of its potential as a mobile diagnostic tool. J Biophotonics. 2020;13(6):e2452. [DOI:10.1002/jbio.201960213]
9. Rajamanickam GP. A multispectral imaging method and device to detect and quantify the presence of fluid in the middle ear to facilitate the diagnosis and triage of ear infections. [Dissertation]. Cambridge, MA: Massachusetts Institute of Technology; 2020.
10. Rosenfeld RM. Diagnostic certainty for acute otitis media. Int J Pediatr Otorhinolaryngol. 2002;64(2):89-95. [DOI:10.1016/s0165-5876(02)00073-3]
11. Valdez TA, Carr JA, Kavanagh KR, Schwartz M, Blake D, Bruns O, et al. Initial findings of shortwave infrared otoscopy in a pediatric population. Int J Pediatr Otorhinolaryngol. 2018;114:15-9. [DOI:10.1016/j.ijporl.2018.08.024]
12. Valdez TA, Spegazzini N, Pandey R, Longo K, Grindle C, Peterson D, et al. Multi-color reflectance imaging of middle ear pathology in vivo. Anal Bioanal Chem. 2015;407(12):3277-83. [DOI:1s00216-015-8580-y]
13. Kapsokalyvas D, Bruscino N, Alfieri D, de Giorgi V, Cannarozzo G, Cicchi R, et al. Spectral morphological analysis of skin lesions with a polarization multispectral dermoscope. Opt Express. 2013;21(4):4826-40. [DOI:10.1364/OE.21.004826]
14. Bae SJ, Lee DS, Berezin V, Kang U, Lee KH. Multispectral autofluorescence imaging for detection of cervical lesions: A preclinical study. J Obstet Gynaecol Res. 2016;42(12):1846-53. [DOI:10.1111/jog.13101]
15. Spigulis J, Oshina I, Berzina A, Bykov A. Smartphone snapshot mapping of skin chromophores under triple-wavelength laser illumination. J Biomed Opt. 2017;22(9):91508. [DOI:10.1117/1.JBO.22.9.091508]
16. Rey-Barroso L, Burgos-Fernández FJ, Delpueyo X, Ares M, Royo S, Malvehy J, et al. Visible and Extended Near-Infrared Multispectral Imaging for Skin Cancer Diagnosis. Sensors (Basel). 2018;18(5):1441. [DOI:10.3390/s18051441]
17. Ortega S, Fabelo H, Iakovidis DK, Koulaouzidis A, Callico GM. Use of Hyperspectral/Multispectral Imaging in Gastroenterology. Shedding Some¯Different¯Light into the Dark. J Clin Med. 2019;8(1):36. [DOI:10.3390/jcm8010036]
18. Kashani RG, Młyńczak MC, Zarabanda D, Solis-Pazmino P, Huland DM, Ahmad IN, Singh SP, Valdez TA. Shortwave infrared otoscopy for diagnosis of middle ear effusions: a machine-learning-based approach. Sci Rep. 2021;11(1):12509. [DOI:10.1038/s41598-021-91736-9]
19. Schmilovitch Z, Alchanatis V, Shachar M, Holdstein Y. Spectrophotometric Otoscope: A New Tool in the Diagnosis of Otitis Media. J Near Infrared Spectrosc. 2007;15(4):209-15. [DOI:10.1255/jnirs.739]

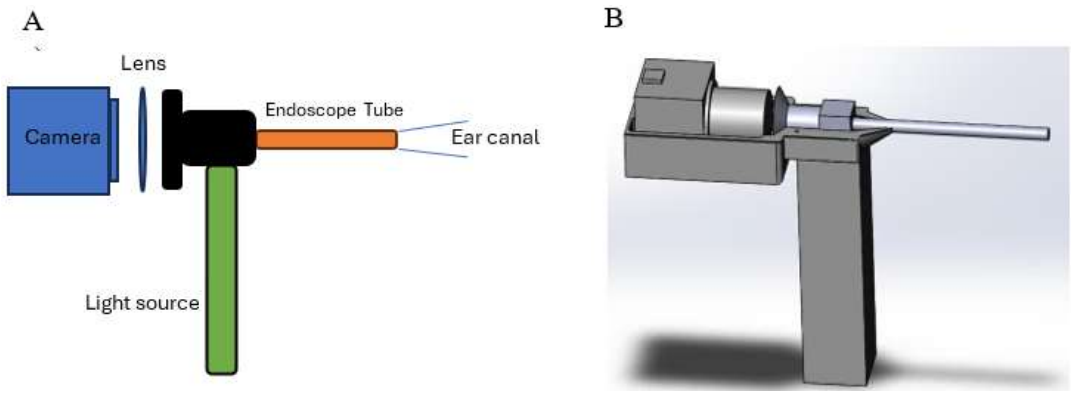

Figure 1. Hyperspectral tympanoscope. **A)** The schematic image of different components of the hyperspectral tympanoscope. **B**) The 3D image of the final hyperspectral tympanoscope.

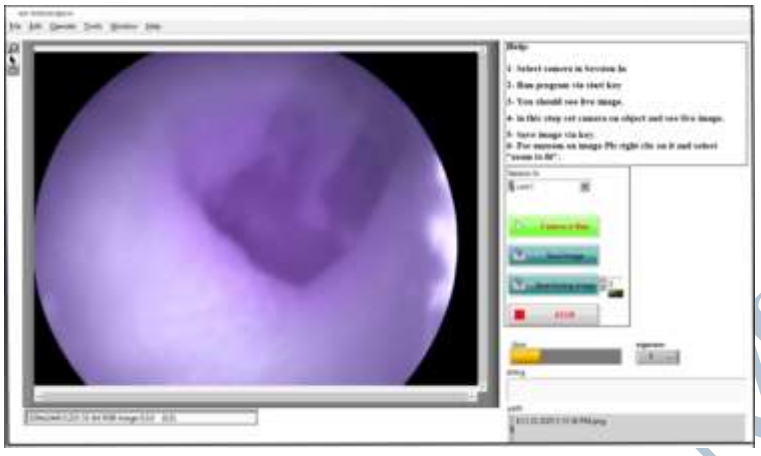

Figure 2. Screenshot of the developed Lab View software

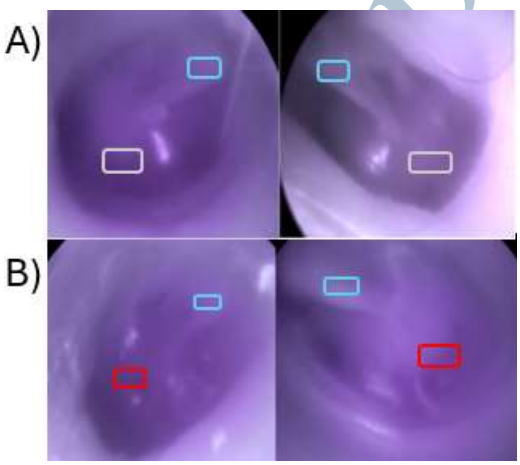

Figure 3. Near-infrared images of normal and abnormal human middle ears. **A)** Near-infrared images of two normal tympanic membranes; **B)** Near-infrared images of two ears with middle ear effusion.

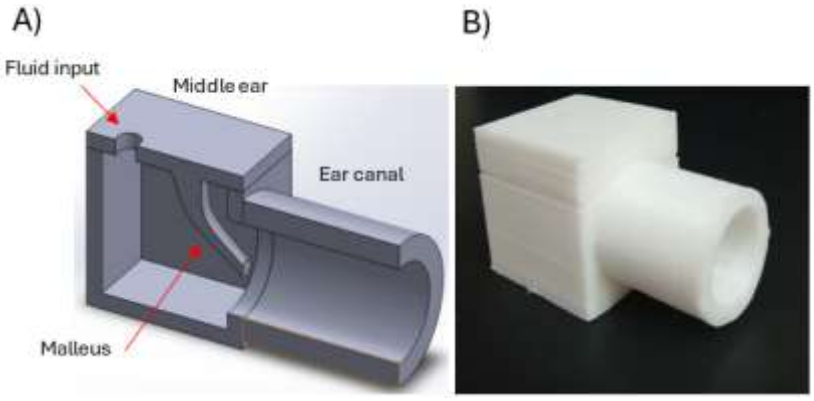

Figure 4. Middle ear-mimicking phantom; **A)** 3D model and **B)** Printed and used in this study.

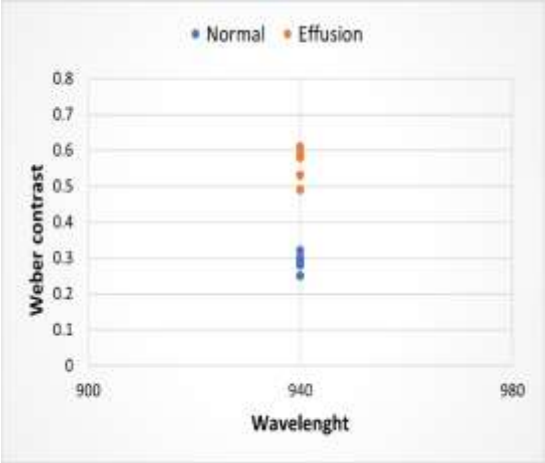

Figure 5. The Weber contrast values for Near-infrared images in five normal children and five children with middle ear effusion.

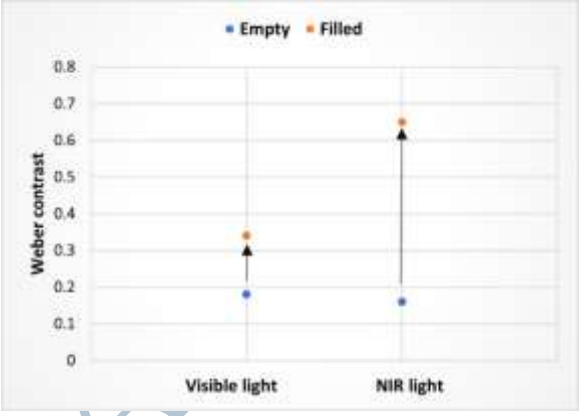

Figure 6. Weber contrast comparison between the empty and filled middle ear-mimicking phantoms with visible and Near-infrared imaging.